Abstract

The Argonne Wakefield Accelerator (AWA) is an experimental accelerator that has achieved record accelerating gradients of 100MV/m. High charge 'drive bunches' excite co-propagating electromagnetic fields in a dielectric structure that can accelerate small 'witness bunches' of electrons that are injected after the drive beam. Producing the drive bunches requires high quantum efficiency (QE) photocathodes to replace the current magnesium photocathode. This report details refinements of the apparatus and procedure for producing Cs_2Te photocathodes, improving their quantum efficiency and uniformity.
To measure the charge coming off the end of the AWA beamline, a fast Faraday cup working in air has been designed and constructed. Tests demonstrate that the Faraday cup has frequency response around 7GHz, resulting in a rise time of 50ps. Such sensitivity should sufficient to distinguish electron microbunches, when the AWA runs in bunch-train mode. The Faraday cup has also been used to take data on the dark current produced by field emission in the RF gun.

Photocathodes and a Faraday Cup for the AWA

Khoo, Teng Jian

August 7, 2008

Contents

1 Introduction **2**

2 Photocathode fabrication **2**
2.1 Motivation . . . 2
2.2 Cs_2Te deposition . . . 3
2.3 QE measurement . . . 4
2.4 Results . . . 5
2.5 Discussion . . . 10

3 AWA beamline Faraday cup **11**
3.1 Cup design and assembly . . . 11
3.1.1 Impedance calculations . . . 12
3.1.2 Assembly . . . 12
3.2 Measurements . . . 13
3.3 Testing . . . 13
3.4 Results . . . 14
3.4.1 TD 540 Scope . . . 14
3.4.2 TD 6154C Scope . . . 16
3.5 Discussion . . . 19
3.5.1 TDS 540 charge measurement . . . 19
3.5.2 TDS 6154C charge measurement . . . 19

4 Summary **23**

5 Acknowledgements **23**

1 Introduction

This is a report on my work at Argonne National Laboratory, as part of the inaugural Lee Teng Internship, from June 2 – August 8 2008. For the internship, I was affiliated with the Argonne Wakefield Accelerator (AWA) group under the High Energy Physics (HEP) division. Under the supervision of Dr. Zikri Yusof, and in collaboration with Adam Clark, I assisted in the fabrication of cesium telluride (Cs_2Te) photocathodes intended eventually for the AWA gun. With the aid of Richard Konecny and Frank Skrzecz, I also helped design, assemble and test a Faraday cup for the AWA beamline.

2 Photocathode fabrication

The development of high quantum efficiency (QE) photocathodes for the AWA gun is an ongoing project for the AWA group. We worked on refining a recipe for Cs_2Te photocathodes, aiming to maximize the overall QE and uniformity of the photocathodes. As the photocathode deposition had to be carried out at pressures under 10^{-9} Torr, I had to learn the fundamentals of operating and handling ultra-high vacuum (UHV) systems, as well as the basic principles of thin-film deposition.

2.1 Motivation

The AWA is an electron accelerator that uses high charge, low-energy 'drive bunches' to accelerate low charge 'witness bunches', for which the group requires a high-current electron source, i.e. a high QE photocathode. The RF gun currently in use incorporates a magnesium photocathode, which has a QE in the range $10^{-6} - 10^{-4}$. This is sufficient to produce individual electron bunches of up to 100nC, but is inadequate for more complex bunch train experiments.

Future goals of the AWA involve producing bunch trains of up to 64 microbunches. This is done by splitting the pulse from the drive laser that illuminates the photocathode. The attainable laser energy per pulse is 10mJ at a photon energy of 5eV. An optimistic loss estimate of 80% before reaching the photocathode gives a pulse energy of 2mJ, or 31.25μJ per micropulse for 64 micropulses. So, to produce 64 microbunches at 50nC each, the QE required would be:

$$\begin{aligned} \text{QE} &= \frac{\text{Number of electrons out}}{\text{Number of photons in}} = \frac{50 \times 10^{-9}}{e} \cdot \frac{5\,e}{31.25 \times 10^{-6}} \\ &= 0.8\% \end{aligned}$$

If we instead wish to produce 16 microbunches at 50nC per bunch, the required QE is 0.2%. On this basis, we would like to fabricate photocathodes with a target QE of at least 1% [1]. Cs_2Te was selected as the photocathode material as it balances high quantum efficiencies (up to 21% at 254nm reported by Loch [2]) with a long lifetime of up to several months.

2.2 Cs_2Te deposition

Our goal was to produce fairly uniform photocathodes with a QE of at least 1% across the entire plug surface. These will eventually be used in a new RF gun that is currently being built for the AWA.

We produced photocathodes via evaporative deposition of tellurium and cesium on a molybdenum plug. The process was carried out at a vacuum pressure of $\sim 10^{-9}$ Torr, with the Mo plug maintained at 130°C. To prevent impurities from accumulating on the surface of the plug, the plug was first shielded while the tellurium and cesium dispensers were heated and allowed to outgas. The shield was then raised to allow tellurium deposition.

Tellurium was deposited on the surface to a thickness of $100-200$Å by heating a crucible containing Te chunks, tracking the thickness of the Te layer using a crystal thickness monitor. The actual Te layer thickness was about 0.6 of the thickness monitor reading.

Once Te deposition was complete, cesium deposition was carried out by evaporating cesium from a chromate dispenser. This involved passing through a current of 5.0A. Measuring the photocurrent produced by a mercury lamp allowed us to track the QE of the photocathode as we carried out the Cs deposition (detailed in the following section). As the rate of increase of QE would plateau after several minutes, we gradually increased the current in steps of 0.25A to approximately 7.0A over the course of the deposition. We ended the cesiation when the QE reached a peak.

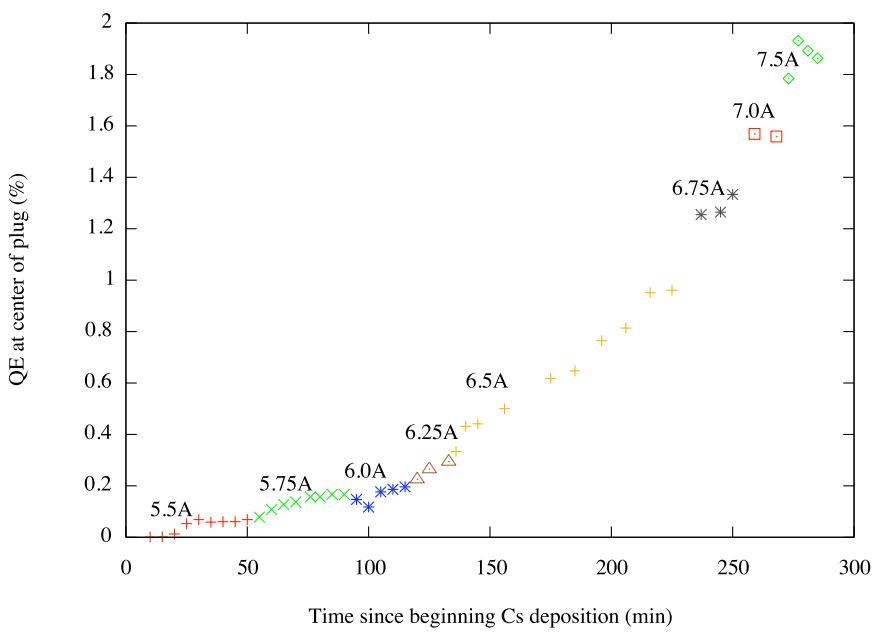

Figure 1: Photocathode deposition on July 23 2008

2.3 QE measurement

Throughout the cesiation, the QE at the center of the photocathode plug was monitored, by measuring the photocurrent produced by a mercury lamp. A filter was used to fix the photon wavelength at 254nm, which is close to the wavelength of the AWA drive laser (250nm), and the intensity of the lamp was kept constant. Photoelectrons from the plug were captured by an anode, biased to 400V, that doubled as a shield for the molybdenum plug. Given the value of the photocurrent and the incident power from the lamp, the QE can be determined to be:

$$\mathrm{QE}(\%) = \frac{I(\mathrm{nA}) \cdot E_{\gamma}(\mathrm{eV})}{P(\mathrm{mW})} \times 10^{-4}$$

Our QE measurements were calibrated by first using a photodiode to measure the incident power from the Hg lamp. We also accounted for the $\sim$10% absorption from the fused silica window through which the light was directed. When deposition was complete, we measured the QE at 5 locations on the photocathode surface, as shown below. Also shown are the positions of the Te and Cs dispensers, in relation to the plug.

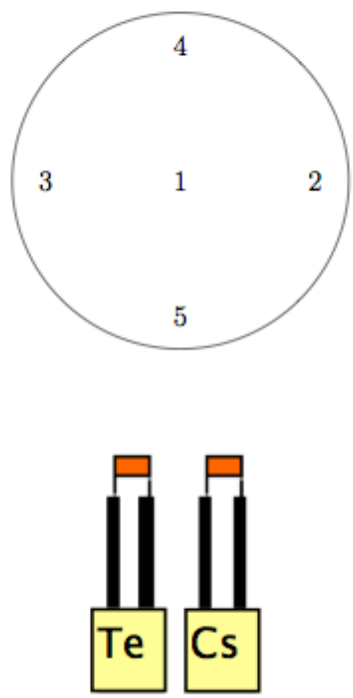

Figure 2: QE measurement positions

2.4 Results

Throughout my time at Argonne, we carried out four depositions, making some adjustments to the photocathode recipe and the apparatus, to optimize the quality of the photocathodes. The first deposition was carried out on June 12 2008. The following table shows the QE variation with time after Cs deposition was ended.

Position	Quantum efficiency			
	0hr	17hr	89hr	113hr
1	0.8%	1.4%	1.2%	1.4%
2	2.5%	3.5%	3.7%	3.3%
3	0.4%	0.6%	0.3%	0.3%
4	1.7%	2.6%	1.3%	1.1%
5	0.5%	0.6%	0.7%	0.8%

Table 1: QE values after deposition on June 12

Clearly, the QE was far from uniform, but we achieved fairly high values of QE in a couple of locations. Two differently colored regions were visible on the plug, roughly corresponding to the regions with higher and lower QE values. Given the pattern of the variation, the reduced QE was believed to be due to the asymmetry in the positioning of the dispensers (the Te dispenser is to the left of the Mo plug, the Cs dispenser to the right). For comparison, a standard Te deposition thickness is 100Å, while the actual Te layer thickness for this deposition was around 150Å (thickness monitor reading: 250Å).

To monitor the degradation of the QE at higher pressures, the chamber was repressurized slowly - the pumps were turned off without opening the chamber. Initially, the QE showed negligible variation as the pressure rose from 2.3×10^{-10} Torr to 3×10^{-6} Torr over the course of three hours. Left overnight, the vacuum chamber came to 9.0×10^{-3} Torr, after which the QE values showed a noticeable drop. The chamber was vented with N_2 gas to 760 Torr, and then pumped back down to 4×10^{-6} Torr. At this point the QE had been significantly degraded.

Position	Quantum efficiency	
	$P = 9.0 \times 10^{-3}$ Torr	After venting
1	0.92%	0.35%
2	1.5%	0.39%
3	0.42%	0.16%
4	0.98%	0.40%
5	0.64%	0.24%

Table 2: QE values before and after venting

A second deposition under the same conditions was carried out on June 25, confirming the pattern of nonuniformity in the QE. The initial pressure was 9.2×10^{-10} Torr. Te was deposited to a thickness monitor reading of 249Å.

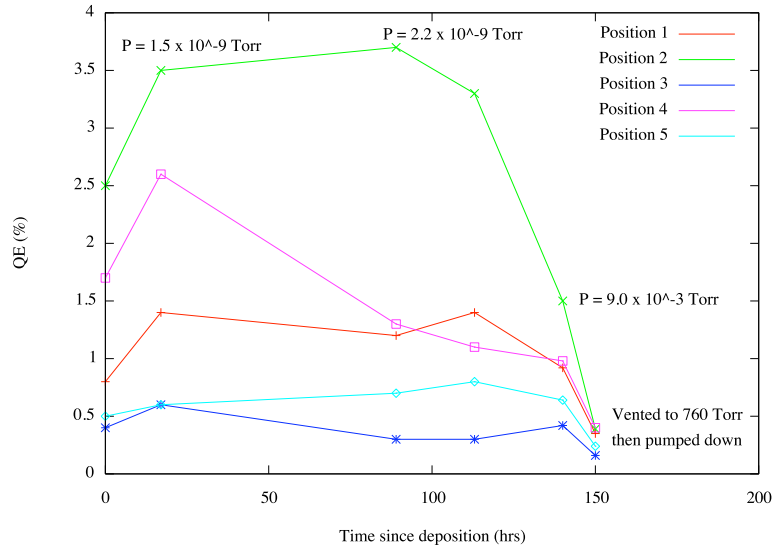

(a) June 12

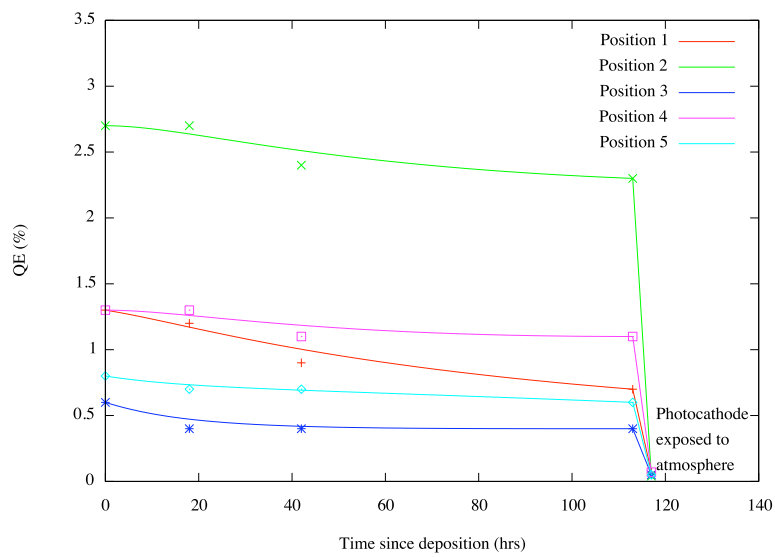

(b) June 25

Figure 3: QE values after deposition on June 12 and 25

Position	Quantum efficiency				
	0hr	18hr	42hr	113hr	After exposure to atmosphere
1	1.3%	1.2%	0.9%	0.7%	0.07%
2	2.7%	2.7%	2.4%	2.3%	0.04%
3	0.6%	0.4%	0.4%	0.4%	0.05%
4	1.3%	1.3%	1.1%	1.1%	0.07%
5	0.8%	0.7%	0.7 %	0.6%	0.05%

Table 3: QE values after the June 25 deposition

To correct the problem, the position of the Te dispenser and the length of a shielding flag on the Cs dispenser were adjusted, and a new deposition carried out on July 9 after refilling the Te dispenser. The starting pressure was 3.6×10^{-9} Torr and the final thickness monitor reading was 200Å.[1] The cesiation was abbreviated, as the goal was to check the uniformity rather than produce a good photocathode.

Position	Quantum efficiency	
	0hr	23hr
1	0.26%	0.21%
2	1.27%	1.23%
3	0.18%	0.30%
4	0.36%	0.35%
5	0.56%	0.3%

Table 4: QE values after deposition on July 9

These results demonstrate a overall increase in the uniformity of the QE, although there remains room for improvement. In particular, only the QE at position 2 differs substantially from the other positions. The shortening of the flag appears to have helped, since visual inspection confirmed that the visible inhomogeneity of the Cs_2Te layer had been reduced to a thin sliver on the right side of the plug corresponding to location 2.

The cesium dispenser shielding flag was shortened further, in the hopes of eliminating the nonuniformity entirely, and another deposition carried out on July 23. Since previous data seemed to suggest that a surfeit of tellurium was reducing our QE, we further reduced the thickness of the Te layer, depositing Te at a rate of 0.1Å/s to a thickness monitor reading of 150Å. This should correspond to a Te thickness of 90Å, if the older calibration remains correct. The starting pressure was 1.3×10^{-9} Torr.

[1] Calibration may have changed due to replacement of tellurium in dispenser.

(a) QE values

Position	Quantum efficiency		
	0hr	18hr	42hr
1	2.65%	1.81%	2.01%
2	3.73%	3.14%	3.33%
3	0.39%	0.69%	0.47%
4	1.76%	1.50%	1.57%
5	1.72%	1.62%	1.18%

(b) QE on the left of the plug

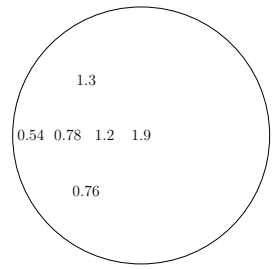

Table 5: July 23 deposition

At first glance, these results do not appear to reflect very substantial improvements in uniformity. However, it is heartening that we have managed to achieve a QE of over 1% for each position on the plug, besides position 3. A more detailed measurement of the QE on the left side of the photocathode shows a marked decrease close to the edge of the plug, which we believe to be due to shadowing effects from the geometry of the chamber. The following diagram shows the drop-off in QE (values shown in percent):

For comparison, average values of QE at the five positions measured for each deposition are plotted on the next page. The first plot is of the actual QE values, while the second shows QE values at each position as fractions of the maximum QE for that deposition (always at position 2).[2]

From the first plot, we see that the QE at position 3, on the left of the plug, furthest from the Cs dispenser, remains almost constant, and never rises above 0.5%. The other QE values, however, show some tendency to increase, particularly positions 1 and 5. Furthermore, other than at position 3, the QE across the photocathode is now above 1%.

The second plot shows more clearly the improvements in uniformity as the shielding flag was shortened. Particularly interesting is that the relative QE of positions 1 and 5 have grown substantially, while the other values have remained roughly constant. Overall, it appears that the vertical nonuniformity has been improved, but the data also strongly indicate a correlation between QE and proximity to the Cs dispenser, which has not been affected much by the changes.

[2]Note: the two June depositions were carried out under nominally identical conditions, while the shielding flag was shortened before each of the July depositions.

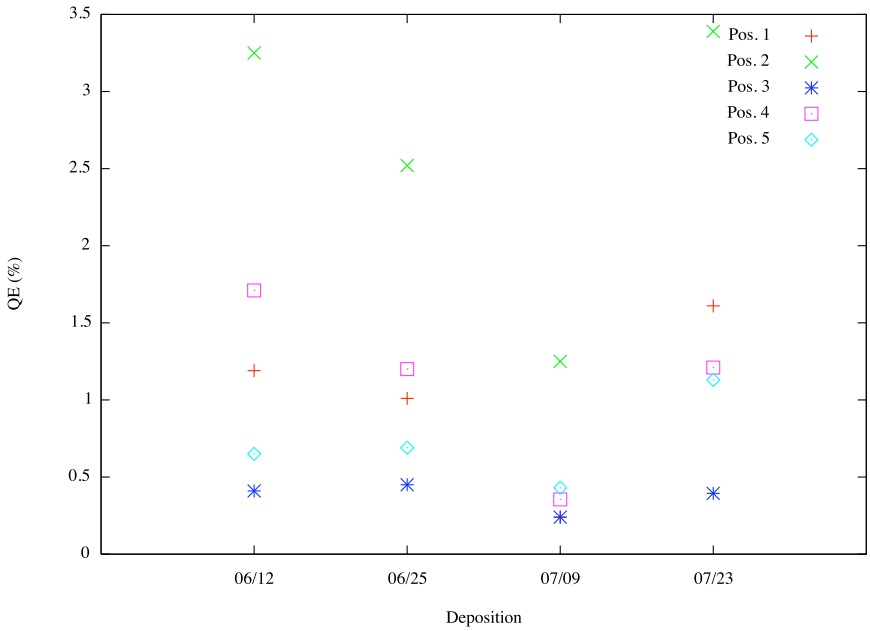

(a) Actual QE values

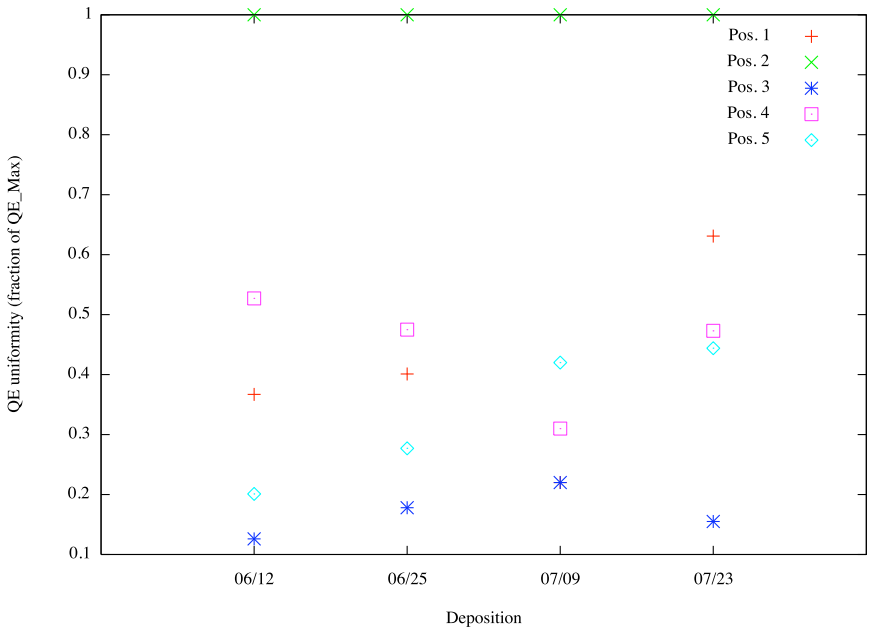

(b) Normalized QE values

Figure 4: Comparison of nonuniformity for depositions from 06/12 to 07/23

2.5 Discussion

Unfortunately, Cs_2Te photocathode fabrication is marked by low reproducibility - the QE achieved tends to vary substantially with each deposition. So, it is difficult to judge precisely the efficacy of our adjustments. Nonetheless, the data point to some limited reduction of nonuniformity in the vertical axis and indicate an effect due to the setup of the deposition chamber, which may be able to be corrected in future. The changes in Te deposition thickness, however, do not seem to have significantly affected the overall QE.

While the present apparatus cannot be changed much beyond further adjusting the shielding flag, a new setup is being designed to deal with the non-uniformity problems. This will allow the Cs and Te dispensers to be placed at the same location during deposition, which should allow a more homogeneous Cs_2Te layer to be formed. The stoichiometry of the photocathode will be refined further.

3 AWA beamline Faraday cup

The objective of this project was to design and build a Faraday cup to serve as a charge measuring device for the electron bunches coming off the AWA beamline. The AWA produces bunches of length 10ps, which are separated by at least 770ps in bunch-train experiments. A major goal is to achieve a time response sufficient to resolve these microbunches. To simplify construction, the cup will be placed outside the vacuum chamber, so the electrons will travel some distance through air before reaching the cup. While this restricts the accuracy of the charge measurements, the ultimate aim of the project is to resolve the electron bunches, which is more dependent on good time response.

3.1 Cup design and assembly

The outer shell was machined from a $6'' \times 4''$ copper cylinder, and the inner conductor from a $5'' \times 1.5''$ copper rod, with the dimensions chosen to provide an impedance $Z = 50\Omega$, matching that of the N-type coaxial connector serving as the output of the deviec. The $2''$ straight segment of the core should be sufficient to stop a 20MeV electron beam [3], and is followed by a tapered section that allows impedance matching with the coaxial connector. The inner conductor is supported by three evenly-spaced nylon screws, and by the central conductor of the coaxial connector.

Other considerations were minimizing the taper angle, so as to reduce ringing and noise in the cup, as well as balance between capturing the entire electron beam and maximizing time-response.

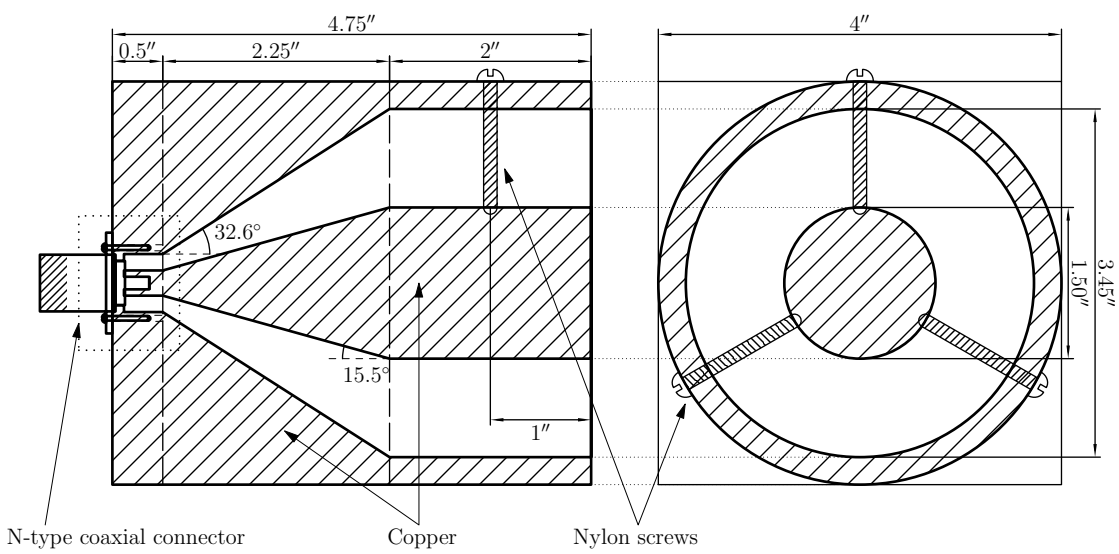

Figure 5: Faraday cup dimensions

3.1.1 Impedance calculations

The impedance for a coaxial line is given by $Z_0 = \frac{1}{2\pi}(\frac{\mu_0}{\epsilon_0})^{1/2}\ln(D/d)$, where μ_0 and ϵ_0 are the permittivity and permeability of free space (valid for air), D and d are the outer and inner diameters of the coaxial line respectively. Matching the chosen impedance of 50Ω gives a ratio D/d of 2.3031. For the taper, the line impedance is given by

$$Z_0 = \frac{1}{2\pi}(\frac{\mu_0}{\epsilon_0})^{1/2}\ln(\frac{\cot(\theta_1/2)}{\cot(\theta_2/2)})$$

where $\theta_{1,2}$ are the half-angles of the inner and outer cones [4]. This is equivalent to maintaining the ratio 2.3031 of the inner and outer diameters. The ratio corresponds to a shell inner diameter $D = 3.45''$ to match the inner conductor diameter $d = 1.50''$ at the front of the conductor. To avoid short-circuits between the inner and outer conductors, the inner conductor tapers to $d = 0.25''$, which gives a shell inner diameter $D = 0.58''$.

3.1.2 Assembly

Assembly of the Faraday cup was very straightforward. Together with the body of the cup, an aluminum plate was machined to help center the inner conductor. The inner conductor is simply placed in the upright outer shell, and rests on the pin of the coaxial connector. This simple setup nonetheless allows sufficiently good electrical contact between the copper and the pin. Placing the aluminum plate around the inner conductor allows precise positioning, and the nylon screws are simply tightened to hold the cup in place.

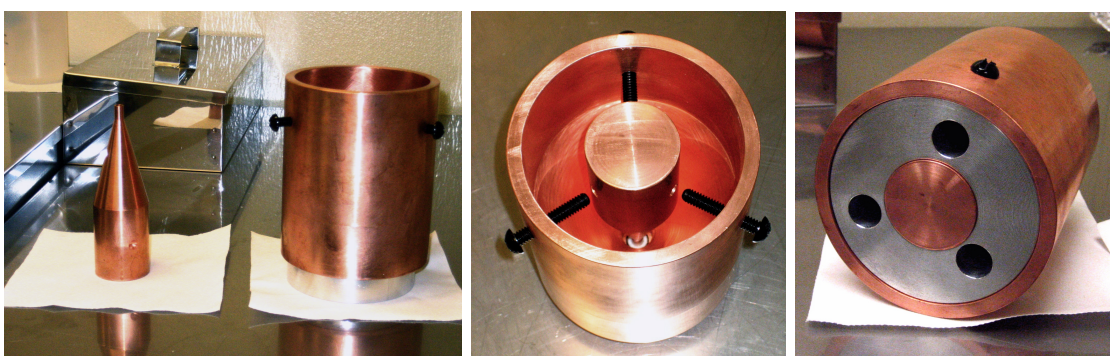

Figure 6: Assembly of the Faraday Cup

3.2 Measurements

The AWA produces electron bunches with charges between 1 and 100nC, and typical bunch lengths between 10 and 30ps FWHM. Based on these details, we can make a rough estimate of the measured voltage between the inner and outer conductors of the Faraday cup. We can treat the cup approximately as a cylindrical capacitor, with a fixed ratio of inner to outer diameter, as determined by the impedance calculations. The capacitance is then given by:

$$C = \frac{2\pi\epsilon_0}{ln(D/d)} \cdot L = \frac{2\pi \cdot 8.85 \times 10^{-12}\text{F m}^{-1}}{0.834} \cdot 0.121\text{m} = 8.04\text{pF}$$

The voltage between the inner conductor and outer shell, $V = Q/C$. If we assume the cup captures all the electrons in a bunch, retaining all the bunch charge long enough for the voltage measurement to be made, we get a calibration of 124V/nC. This assumption is reasonable for the short bunch lengths we intend to measure. However, electron losses from scattering and attenuation within the coaxial cable may substantially reduce the actual measured voltages.

3.3 Testing

The AWA was run on June 21 and 22 with the Faraday cup positioned at the end of the beamline. The cup was connected to a grounding strip, and its output was recorded on an oscilloscope. The AWA beamline contains six YAG panels that can be lowered to intercept the beam. These panels fluoresce when hit by the beam, and thus can be used to track the trajectory and focusing of the beam. A strip of frosted glass placed in front of the Faraday cup allowed the beam to be guided all the way to the cup, using Čerenkov radiation to image the beam. This strip was removed before data were taken. Data were taken with a 500MHz Tektronix TDS 540 oscilloscope, and a faster 15GHz TDS 6154C scope, both with the drive laser activated ('Regular operation') and deactivated ('Dark current').

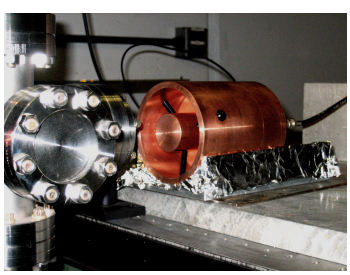

(a) Faraday cup positioned on the beamline

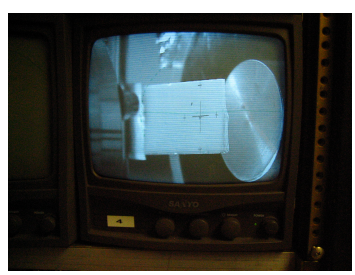

(b) Frosted glass strip to monitor beam reaching cup

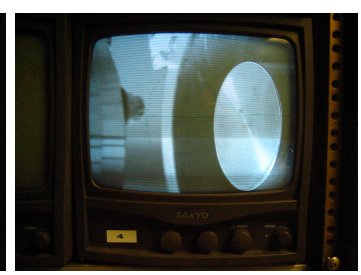

(c) The glass strip was removed before data collection

3.4 Results

3.4.1 TD 540 Scope

Initial tests were made using a TDS 540 scope, with an attenuation of 13dB. Simultaneously measured on the scope were the readouts from two integrated current transformers (ICTs) placed along the beamline. The nominal sampling interval from the scope was 400ps, but given the scope bandwidth, the actual resolution should be about twice that.

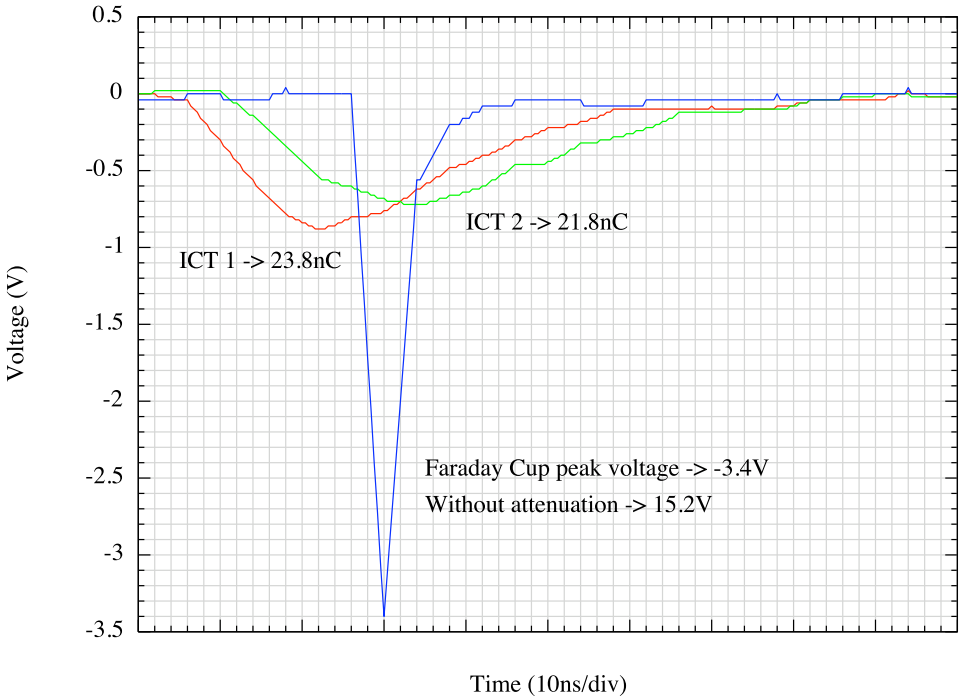

Figure 7: Regular operation on TDS 540

The observed full width at half-max (FWHM) in this trace is 4ns, which is far greater than the length of the electron bunch ($\sim$ 10ps). This is nonetheless much better than the 30ns FWHM of the ICTs. A noticeable feature of the Faraday cup signal is the distortion of the tail of the signal, potentially the effect of ringing or interference in the cup.

The TDS 540 scope was also used to measure the signal of the dark current produced by field emission from the photocathode. The RF gun pulses at 1.3GHz, with a pulse length of 6μs. Two plots are shown: the first was taken with the laser off and a focusing solenoid deactivated, so the dark current did not reach the end of the beamline. Any signal is the result of RF interference. The second has the focusing solenoid on, and a small dip is clearly visible in the Faraday cup trace.

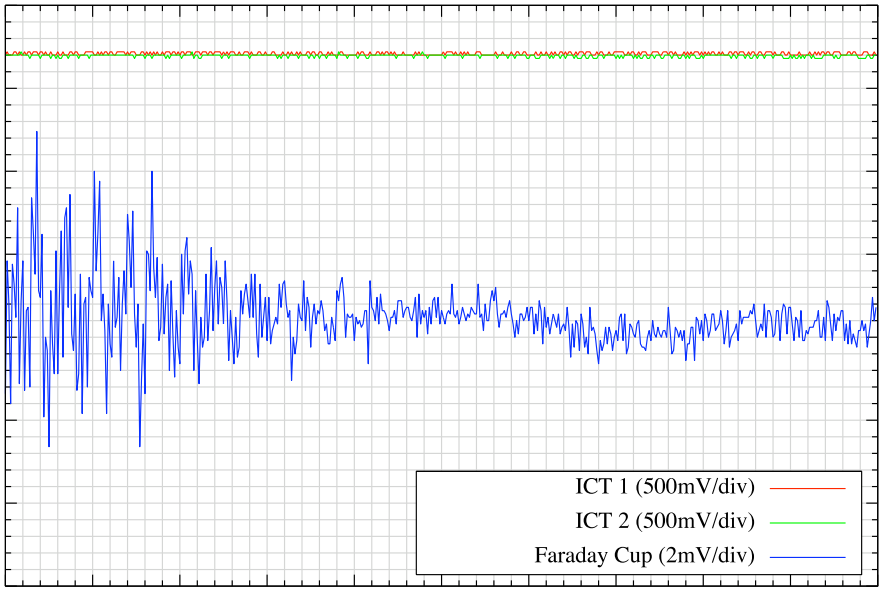

Time (1 microsecond/div)

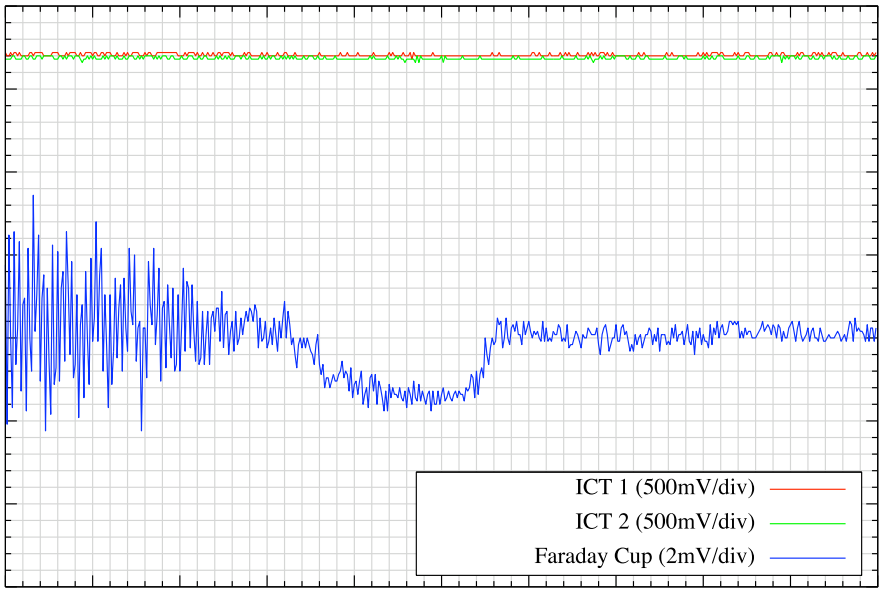

Time (1 microsecond/div)

Figure 8: Dark current on TDS 540

3.4.2 TD 6154C Scope

Data were taken also using a TDS 6154C scope, with an attenuation of 60dB. The nominal sampling interval from the scope was 25ps.

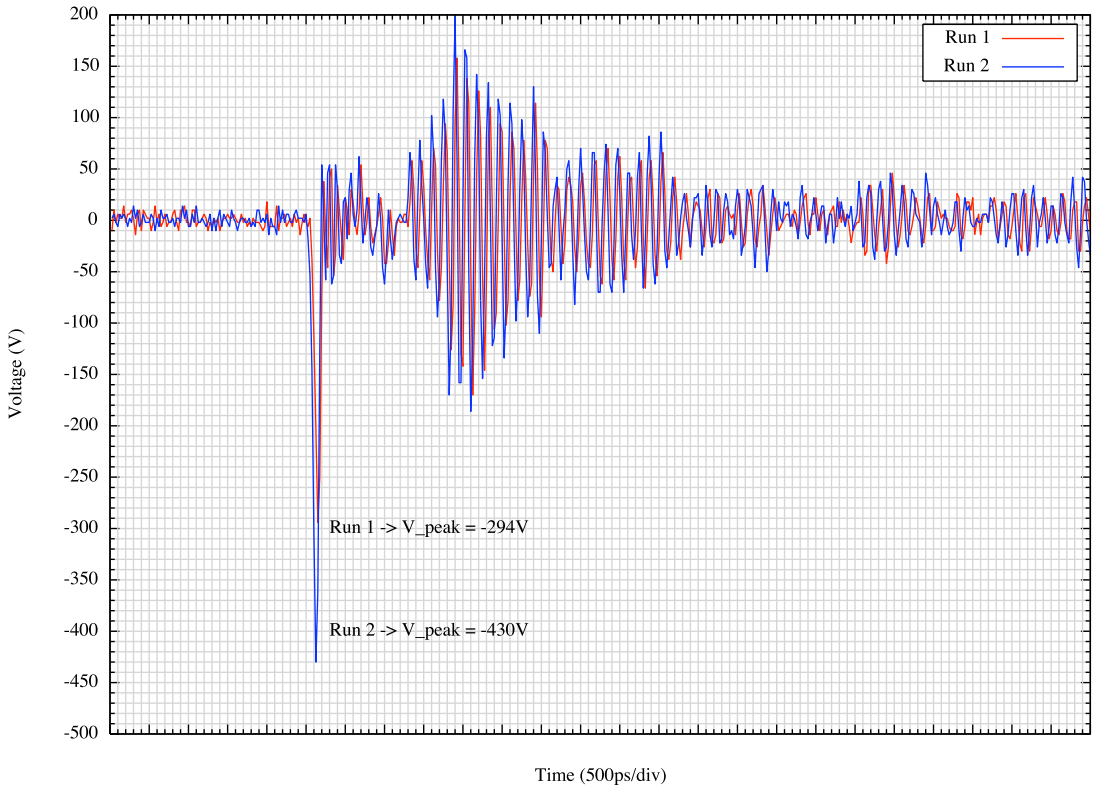

Figure 9: Regular operation on TDS 6154C

The faster scope demonstrates that the Faraday cup is at least sensitive enough to discern pulses on the scale of 100–200ps. We can see a clear spike from the arrival of the electron bunch, followed by a good deal of noise, which appears to have a characteristic shape. Possible sources of the noise are X-rays and other radiation produced by bremsstrahlung and secondary emission in the cup, as well as reflection of the signal due to imperfect impedance matching. Essentially no RF interference was observed on this timescale.

The dark current signal on the fast scope is quite noisy, but some details can be discerned, in particular an oscillatory section about 1μs in, and a later spike at the 9μs mark.

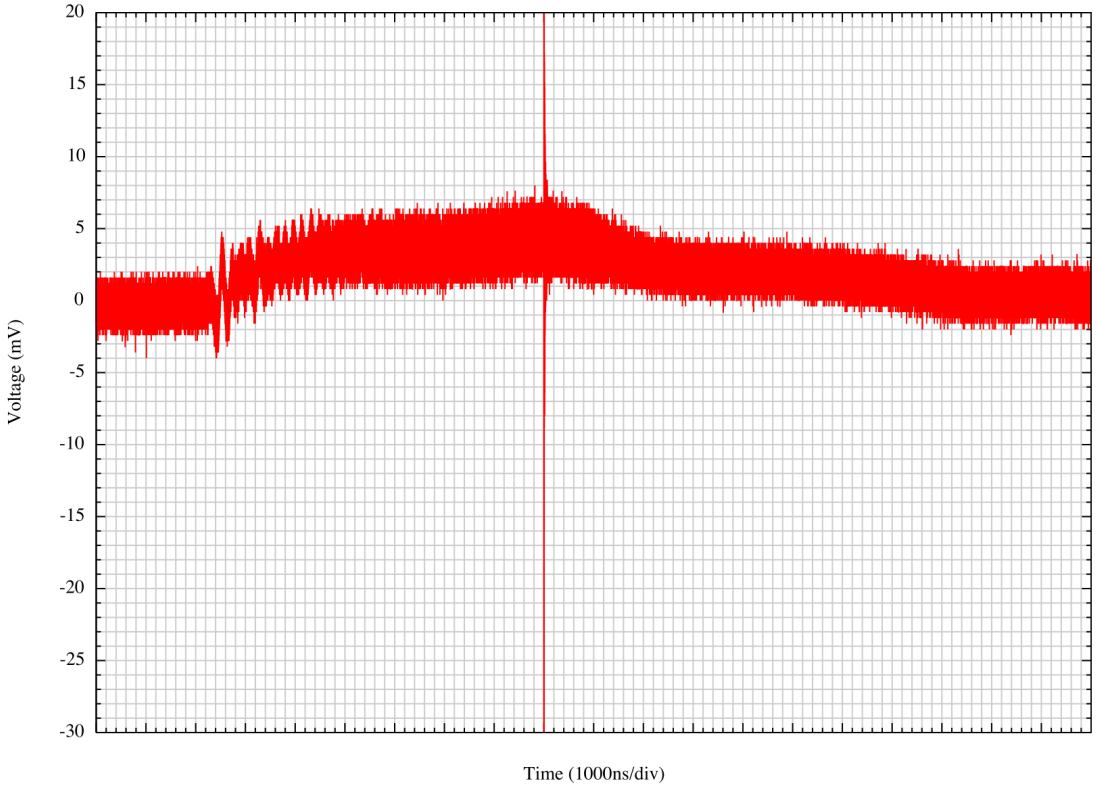

Figure 10: Dark current on TDS 6154C

Zooming in on the spike in the region from 8998.5–9011ns reveals a great deal of structure. There is a clear correspondence with the 'Regular operation' traces. The signal is diminished, but otherwise the features are exactly reproduced. In the plot on the following page, the 'Run 1' and 'Run 2' signals have been divided by a factor of 3.

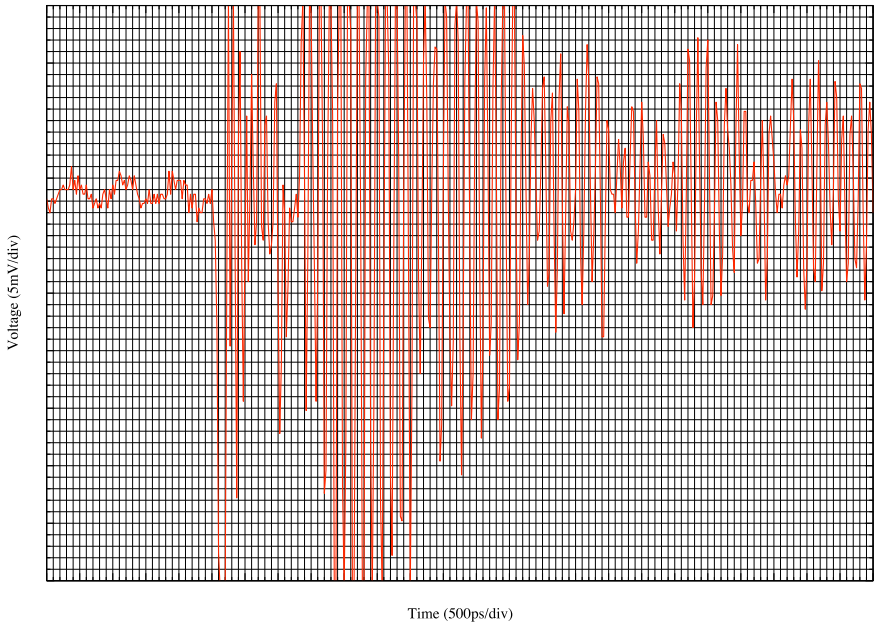

(a) Dark current alone

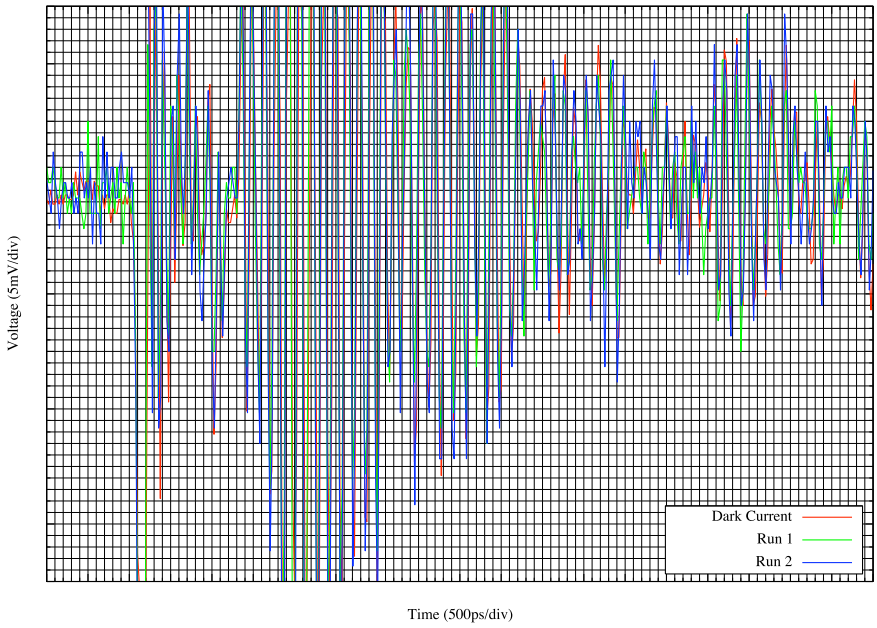

(b) Dark current with photocurrent signals

Figure 11: The dark current signal matches the photocurrent signal here.

3.5 Discussion

Our goal for the Faraday cup is to be able to measure the charge of each electron pulse with a good time resolution. Determining the calibration of the Faraday cup requires knowing the charge of each pulse measured. We first consider the results from the TDS 540 scope.

3.5.1 TDS 540 charge measurement

The signals from ICT 1 and 2 have calibrations of 37mV/nC and 33 mV/nC respectively, translating to measured charges of 24nC and 22nC. The Faraday cup signal has a peak voltage of 13V, after accounting for the 13dB attenuation (See figure 7). This is small given the theoretical calibration of the cup. However, this is not unexpected, as magnet problems and lack of diagnostics at the end of the beamline made beam transport poor. Other factors for the reduction include scattering of the electrons and losses in the cable, which was rated only to 6GHz [5].

3.5.2 TDS 6154C charge measurement

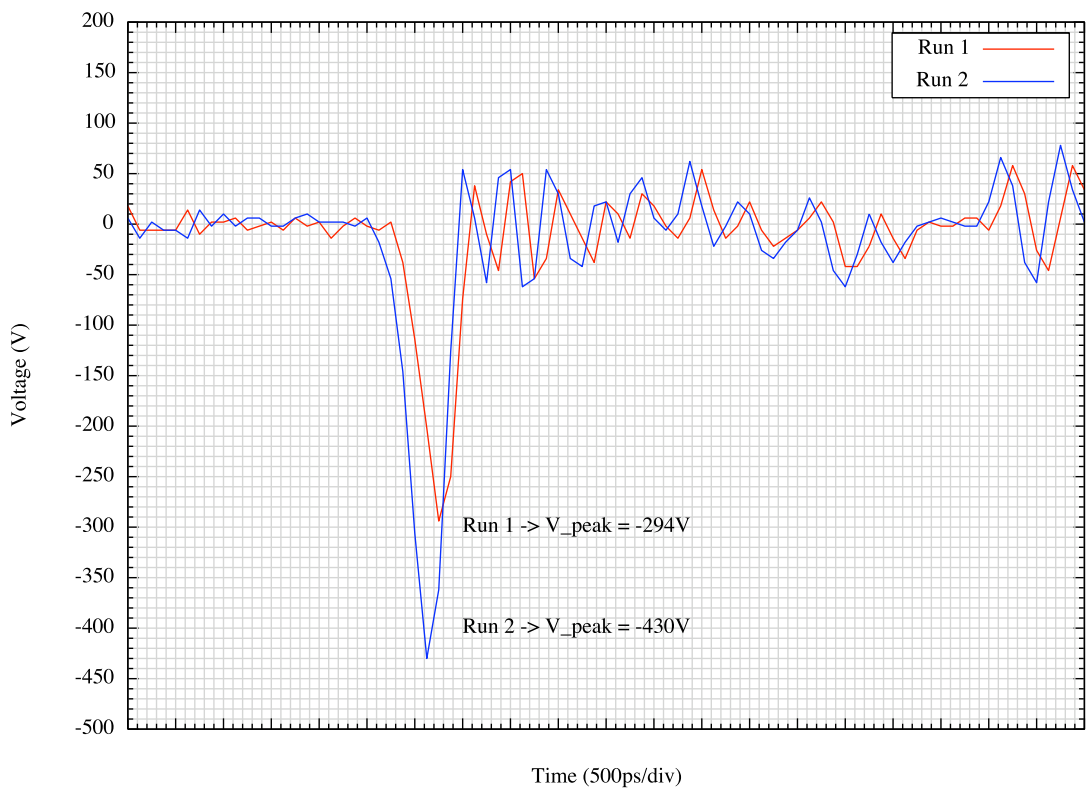

Figure 12: Fast scope traces of the main voltage spike

For the fast scope runs, we measured peak voltages of 294V and 430V, after accounting for the 60dB attenuation applied. These measured voltages correspond to bunch charges of 2.4nC and 3.5nC respectively. The full width at half-max (FWHM) of the voltage spike is about 80ps.

For comparison, the ICT pulse traces were recorded for run 2, as shown in figure 13. The peak voltages of 1050mV and 940mV, for ICT 1 and 2 respectively, put the bunch charge at 28.5nC, slightly more that the bunch charge for the slow scope runs.

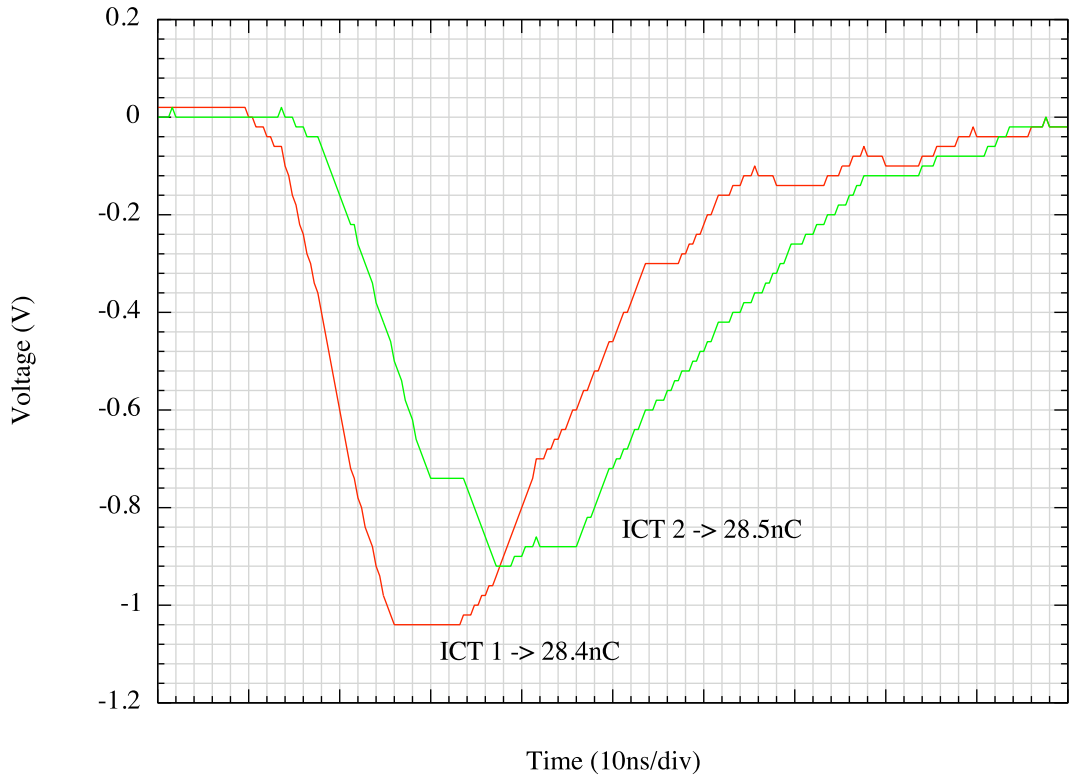

Figure 13: ICT pulses for run 2 on the fast scope

Taking the FFT of the fast scope traces reveals a clear peak at around 7GHz, which corresponds to a rise time $t_r = 0.35/\mathrm{BW} \simeq 50\mathrm{ps}$. This agrees well with the observed rise time. When bunch train experiments are run in the AWA, the 10ps bunches are separated by the RF period of 770ps, so this time response should certainly be good enough to resolve the microbunches.

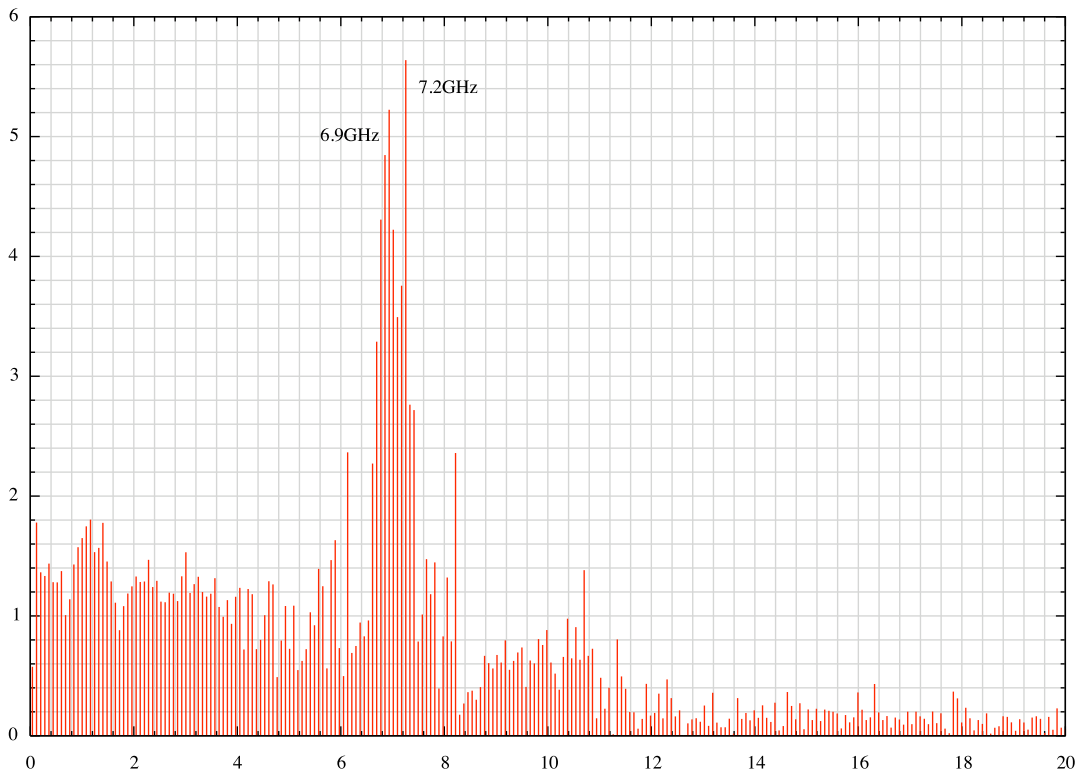

Figure 14: FFT of fast scope trace

The cable used to connect the Faraday cup to the fast scope was a 1/4" FSJ 1-50 coaxial cable (Brand: Andrew Heliax). On the next page is shown a plot of the attenuation at various frequencies, using data supplied by the manufacturer [6]. An estimate of 100 feet for the length of the cable is reasonable,and would diminish the signal by a factor of 7.5 at 7GHz, placing the charge from the Faraday cup at 26.3nC for run 2, or 92% of the ICT signal. If the exact length of the cable can be determined, it may be interesting to try and regenerate the original signal.

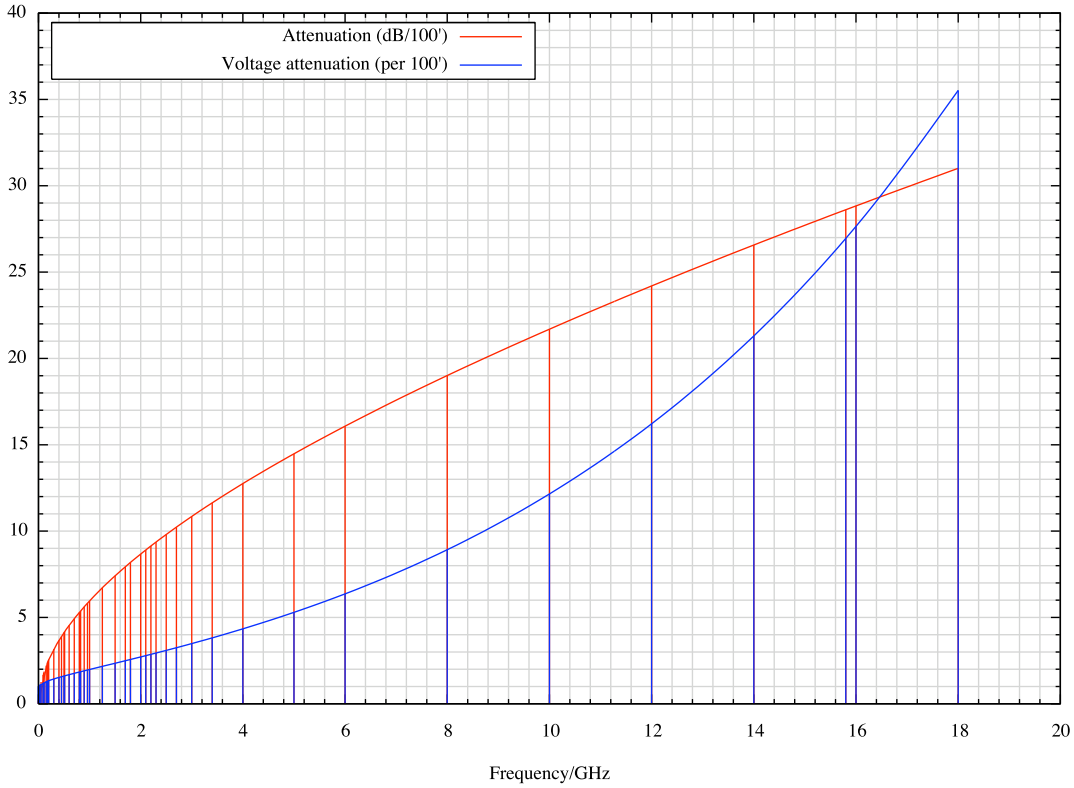

Figure 15: Attenuation in 1/4" FSJ 1-50 coaxial cable

Overall, our initial results from the Faraday cup seem promising, however some testing remains to be done, and the current setup can be improved. Specifically, the grounding of the cup can be improved so as to reduce noise from reflections of the signal, and the calibration of the cup can certainly be improved. Multibunch experiments will be conducted in the near future, to confirm whether the cup is capable of resolving microbunches. Further analysis of the dark current data is necessary, and other sources of noise and attenuation, such as scattering in the quartz window and off the surface of the cup may also be able to be characterized.

4 Summary

Cesium telluride photocathode production for the AWA is underway, and has been refined via adjustments of the apparatus and methods. The shortening of a shielding flag for the cesium dispenser has resulted in some small gains in QE uniformity. However, substantial nonuniformity remains, and is believed to be due to the placement of the Cs dispenser in the deposition chamber, and possible shadowing effects affecting the Te deposition. Further refinements to apparatus and process are intended to help produce even better quality photocathodes.

A copper Faraday cup for the AWA beamline has been built and tested, showing time response that should be sufficient to distinguish individual electron microbunches (bunch length $\sim$ 10ps)in bunch-train experiments. The cup has frequency response of around 7GHz, corresponding to a rise time of 50ps. This resolution is sufficient to resolve individual microbunches when the AWA runs in bunch-train mode. Calibration of the Faraday cup is ongoing, as are analyses of dark current data taken by the cup.

Future plans for the Faraday cup include testing on multibunch experiments, as well as improvements in the setup to reduce noise levels.

5 Acknowledgements

My deepest appreciation goes to Zikri Yusof for taking me on as an intern, and for instructing me in the proper ways of handling ultra-high vacuum systems and thin-film deposition procedures. It goes without saying that if not for him, none of this work would have been possible. Richard Konecny's knowledge and experience was invaluable for the work of designing the Faraday cup, and Frank Skrzecz was similarly indispensable for actually machining the material for the cup. Thanks are also due to Adam Clark for livening up the experience of this internship, and to John Power, Manoel Conde and the other members of the AWA group for their assistance and hospitality in hosting me as an intern. Finally, the support and company of the other Lee Teng Interns and other ANL summer students was memorable and much appreciated.

References

[1] Discussions with Zikri Yusof, AWA Group, HEP Division,
Argonne National Laboratory.

[2] R.A. Loch: *Cesium-Telluride and Magnesium for high-quality photocathodes*,
Master's thesis, University of Twente, the Netherlands (2005).

[3] Discussions with Richard Konecny, AWA Group, HEP Division,
Argonne National Laboratory.

[4] M.S. Zucker and J.W. Bittner:
A Faraday cup with high frequency response for a 200MeV LINAC proton beam,
IEEE PAC 1991.

[5] Huber + Suhner AG: *Data Sheet – Coaxial Cable: RG 223 U*
referenced at http://www.repic.co.jp/contents/products/huber/seihin/rf/pdf/rg223u.pdf

[6] Commscope Product Specifications: *FSJ1-50A*
referenced at http://awapps.commscope.com/catalog/pdf/FSJ1-50A.aspx?id=1342